Chemical Physics Impact 8 (2024) 100566

Contents lists available at ScienceDirect

Chemical Physics Impact

journal homepage: www.sciencedirect.com/journal/chemical-physics-impact

Full Length Article

Structural, optical and electrochromic properties of WAW films for profound electrochromic applications deposited by DC & RF magnetron sputtering

K Naveen Kumar [a,b,*], Habibuddin Shaik [a,b], Sheik Abdul Sattar [a], Ashok Reddy G V [a], Ramanadha Mangiri [c], R Imran Jafri [d], R. Premkumar [e], R. Govindharaju [f], B. Mary Juliet [f], Sabah Ansar [g]

[a] Department of Physics, Nitte Meenakshi Institute of Technology, Yelahanka, Bengaluru, 560064 India
[b] Centre for Nano-materials and MEMS, Nitte Meenakshi Institute of Technology, Yelahanka, Bengaluru, 560064 India
[c] Department of Energy Systems Engineering, Seoul National University, Seoul, 08826, Republic of Korea
[d] Department of Physics and Electronics, Christ University, Hosur Road, Bengaluru, 560029 India
[e] Department of Physics, N.M.S.S.V.N. College, Nagamalai, Madurai 625019, Tamil Nadu, India
[f] Department of Chemistry, Thanthai Hans Roever College (Autonomous), (Affiliated to Bharathidasan University, Tiruchirappalli), Perambalur 621 220, Tamil Nadu, India
[g] Department of Clinical Laboratory Sciences, College of Applied Medical Sciences, King Saud University, P.O. Box 10219, Riyadh, 11433, Saudi Arabia

ARTICLE INFO

Keywords:
Electrochromism
$WO_3/Ag/WO_3$ (WAW)
Tungsten oxide (WO_3)
Sputtering and colorationefficiency

ABSTRACT

One of the most frequently used transition conducting oxides (TCO) is indium tin oxide. Indium is very expensive because of the lack of availability. So Most of the researchers focused on cost-effective materials and they have developed Dielectric/Metal/Dielectric (DMD) structures for ITO-free applications. Examples of dielectric materials are AZO, MoO_3, TiO_2, and WO_3. The dielectric material is sandwiched between metals such as Au, Ag, Pt, Cu, and Al. The efficacy of these DMD structures is purely based on the thickness of the dielectric and metal layers. Once the metal layer thickness is more than 15 nm, the transmittance is much less due to the thickness of the material and it will work as a reflector. Moreover, as WO_3 is the most widely and frequently used material we focus on the fabrication of $WO_3/Ag/WO_3$ (WAW) for replacing TCO in the electrochromic device and making it indium-free. WAW structures are widely used in smart windows, gas sensors, solar cells, photodetectors, etc. For electrochromic applications, these WAW structures showed good transmittance, fast switching speed, best coloration efficiency, and best optical modulation in comparison to WO_3/ITO structure and are also cost-effective.

1. Introduction

Indium Tin Oxide (ITO) is one of the most frequently used TCO materials. High electrical conductivity and transmittance are the major requirements for an ideal transparent conducting electrode (TCE) application such as touch panels, organic light-emitting diodes, gas sensors, flat panel displays, solar cells, plasma displays, etc.[1]. An ideal TCO should have low resistivity and optical transmittance of 80% or more in the range of 400 to 800 nm [2]. Different metal oxide semiconductors like SnO_2, TiO_2, ZnO, and In_2O_3 have been used to fabricate transparent conducting oxide (TCO) thin films [3]. The most common TCO are semiconductor metal oxides with large bandgaps such as zinc oxide, tin oxide, indium oxide, and cadmium doped with group III (Al) [4–8], B [9], Ga [10]or group VII (F [11], Cl [12]. These elements have low resistivity and maintain high transmittance in the visible range. Amidst all, Indium tin oxide (ITO) is the most frequently used Transparent conducting oxide (TCO) material. However, it is rarely available and hence expensive. To overcome this problem researchers are dedicated to finding new transparent conductive electrodes such as nanowires, nanotubes, dielectric-metal-dielectric (D/M/D), graphene, and related structures. Amidst sandwiching a thin metal layer between two dielectric layers D/M/D has been recently introduced as an ideal

* Corresponding author.
E-mail address: naveenkilari95@gmail.com (K.N. Kumar).

https://doi.org/10.1016/j.chphi.2024.100566
Received 31 December 2023; Received in revised form 1 March 2024; Accepted 10 March 2024
Available online 11 March 2024

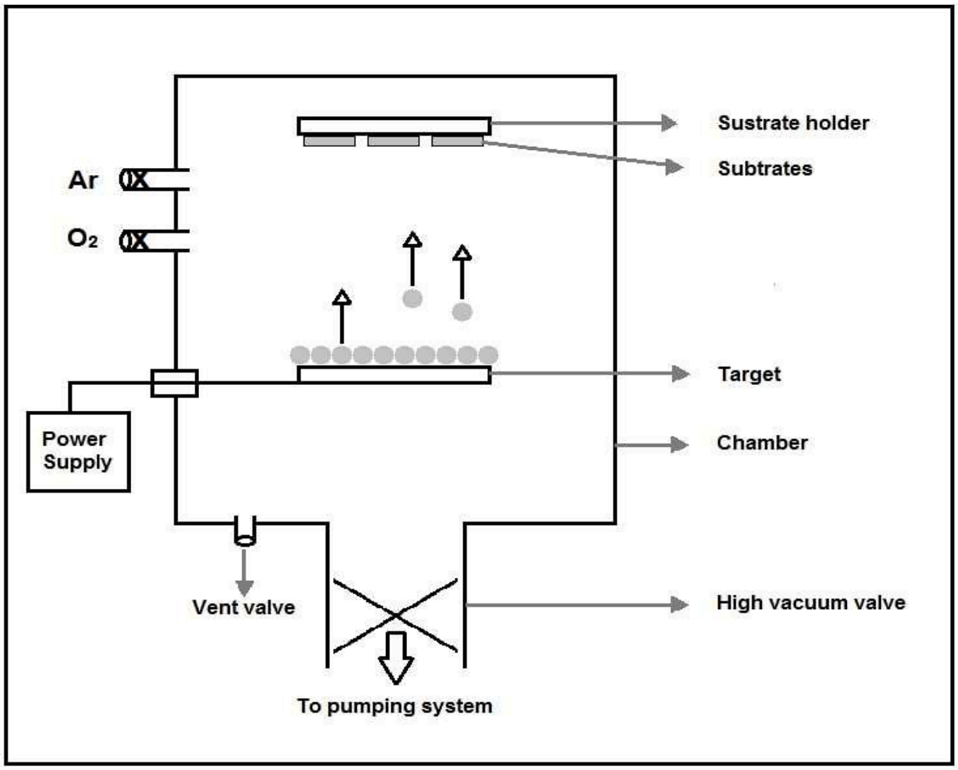

Fig. 1. Schematic representation of Sputtering System.

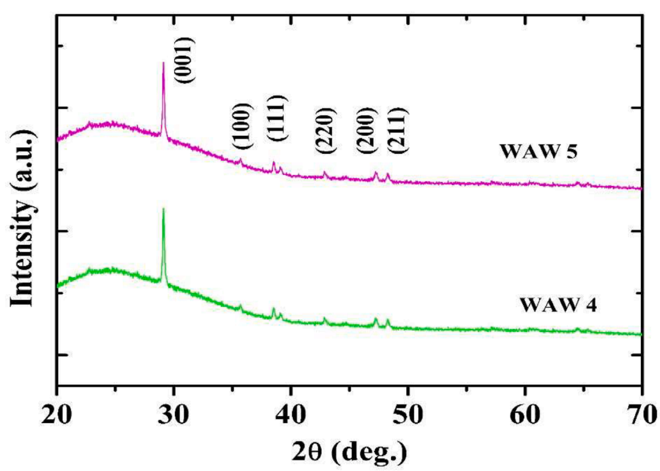

Fig. 2. XRD plots of WAW 4 and WAW 5 strucutre.

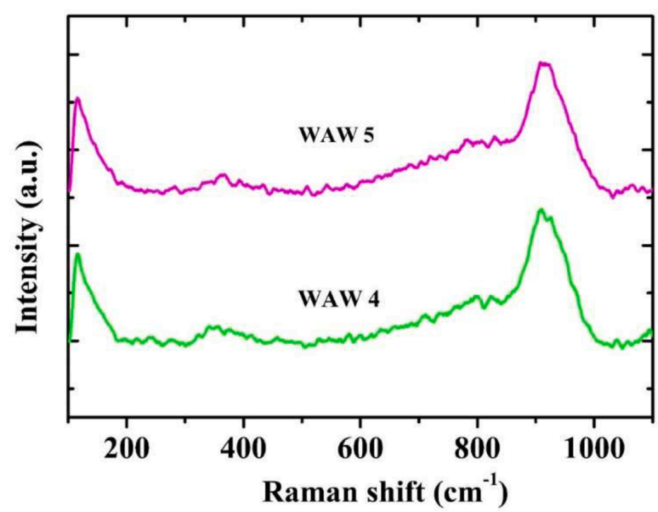

Fig. 3. Raman analysis of WAW 4 and WAW 5 structure.

alternative approach to obtain the combined benefits of high transmission as well as excellent conductivity [13,14]. The efficacy of multilayer transparent DMD structures is dependent on the optimization of the thickness of the dielectric and metal layers [15].

Xuanjie Liu et al. designed flat panel displays with a multilayer structure of ZnS/Ag/ZnS. The electrical and optical performance of the device depends on the thickness of the silver layer approximately 12 nm [16]. For the electrochromic applications, various structures of DMD are there, such as MoO_3/Ag/MoO_3 [17], TiO_2/Ag/TiO_2 [18], and WO_3/Ag/WO_3 [19]. Among these DMD structures, the WO_3/Ag/WO_3 structure is the best for electrochromic applications.

For the electrochromic applications, we have several electrochromic materials. These materials are classified into organic and inorganic materials. Inorganic materials such as TiO_2 [20], NiO [21], V_2O_5 [22], WO_3 [23–25] and organic materials are viologens [26], poly (3,4 ethylene dioxythiophene) (PEDOT) [27], polyaniline (PANI) [28]. Among all materials, inorganic material tungsten oxide (WO_3) has a quick response, good optical transmittance, long life, coloration efficiency, a wide bandgap, and good semiconductor properties. It is best for electrochromic applications and gas sensors [29]. WO_3 films also possess photochromic [30], gasochromic [31], and good hydrophilic [32] properties. The first electrochromic study on WO_3 was reported in 1969 [33]. In the preparation of WO_3 thin films, several deposition methods are there, they are electron beam evaporation [34–36], thermal evaporation [37,38], DC and RF magnetron sputtering [39–58], hydrothermal methods [59–66], plasma spraying method [67], and sol-gel method [68]. With above stated physical vapor deposition techniques we first try to optimize the thickness of WO_3 to realize DMD structure by

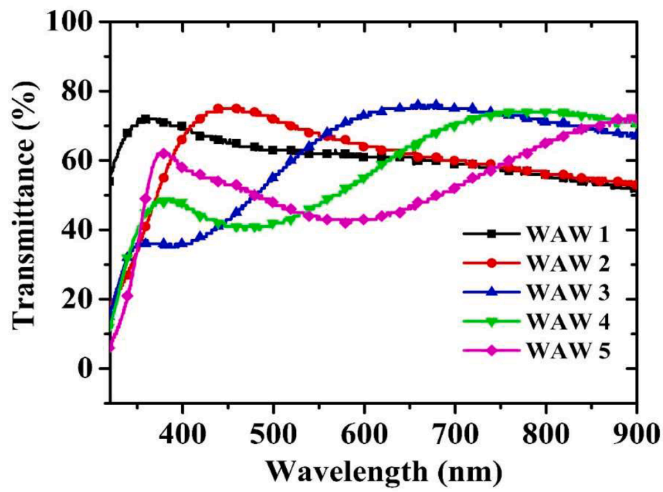

Fig. 4. The optical transmittance of WAW structure with different thicknesses.

incorporating WAW configuration.

WAW is not only for electrochromic applications but also for solar cells [69] and light-emitting diodes[70]. In transparent conducting DMD structures, the major role is played by the thickness of the metal layer. The metal layer could be of Al, Cu, Au, Pt, and Ag. In higher thickness, these metals work as reflectors. The preferred thickness of the metal layer is around 10 to 20 nm. In this range, the metal layer works as transparent and conducting material. Amidst all metals, Ag exhibits the best conducting and photodetector characteristics and is lower in work function compared to other metals [2].

The aim of this study is to develop the indium-free transparent electrode WO_3/Ag/WO_3 (WAW) thin film for electrochromic applications because of the lack of availability of the Indium tin oxide (ITO) and its cost. In this structure, we have varied the thickness of the bottom and top layers of WO_3 thin film thickness and we have kept the metal layers' thickness constant as Ag (12 nm), and W (3 nm). The WO_3 films and Ag films were deposited on the coring glass by using DC and RF magnetron sputtering. The structural, optical, and Electrochromic properties of WO_3 thin films were discussed.

2. Materials and experimental method

2.1. Materials used

The specifications of the corning glass are pre-cleaned 28,947–75 × 25 mm, thickness 0.96 to 1.06 mm from Corning Incorporated, USA. The DI water, H_2SO_4, soap solution, and beakers, were purchased from the Vasa scientific Bangalore, India. Hg_2/$HgCl_2$ and platinum wire were purchased from Sinsil International Pvt Ltd, Bangalore, India. Argon gas (99.999%) and Oxygen gas (99.999%) gas cylinders were purchased from the Bhuruka gas agencies, in Bangalore, India. A pure 3-inch dia tungsten (W) and Silver (Ag) metallic disk were purchased from the scientific and analytical instruments, in New Delhi, India.

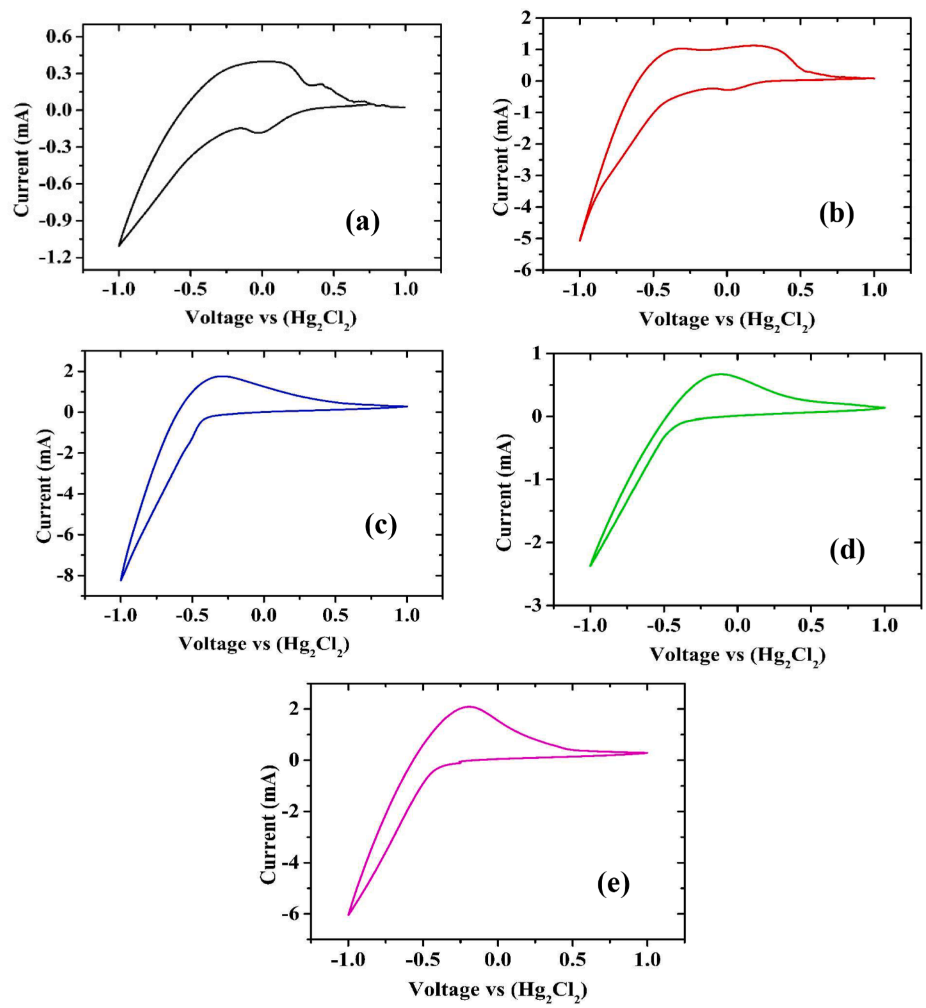

Fig. 5. CV plots of (a) WAW 1, (b) WAW 2, (c) WAW 3 (d) WAW 4 and (e) WAW 5 structure.

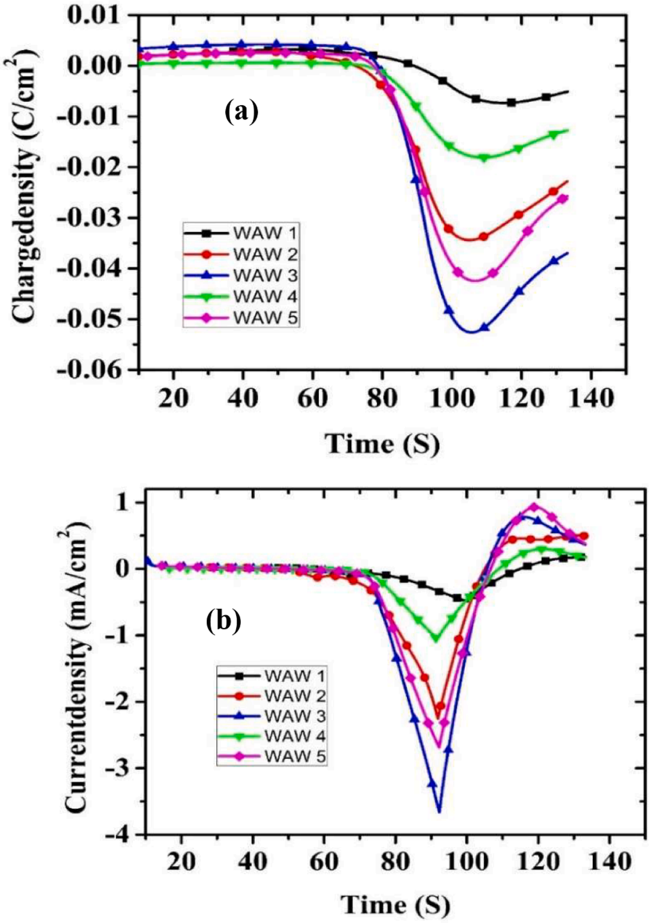

Fig. 6. (a) Charge density, and (b) Current density vs time plots of WAW structure.

2.2. Experimental method

Indium-free transparent electrochromic material was deposited as a WO_3/Ag/WO_3 thin film structure at room temperature using RF and DC magnetron sputtering. These thin films are deposited on corning glass substrates. The sputtering chamber was evacuated 1×10^{-6} mbar by using the mechanical pump as a Rotary pump (up to 1×10^{-3} mbar) and the backing pump as a turbo molecular pump (up to 1×10^{-6} mbar). Inside the chamber pressure was measured using penning and pirani gauges. Before loading the substrate inside the chamber substrates were cleaned ultrasonically following soap solution, DI water and dried with nitrogen gas. A pure 3-inch dia tungsten (W) and Silver (Ag) metallic disk were used. In this work, we have used pure Argon gas (99.999%) as a sputtering gas with a flow rate of 25 SCCM and oxygen gas (99.999%) as a reactive gas with a partial pressure of 8×10^{-4} mabr. For the deposition of tungsten oxide (WO_3) and Silver (Ag) thin films, the distance between the substrate and the target was maintained at 9 cm and 7 cm respectively. The WO_3 and Ag thin films were coated using DC and RF magnetron sputtering respectively. For every deposition before W and Ag metal targets were presputtered in the Argon environment for 10 min and 2 min to remove the adsorbed contaminations from the targets. The Schematic representation of the sputtering system is shown in Fig. 1. The films with pattern of WAW 1 (WO_3/Ag/W/WO_3, 25/10/3/25 nm), WAW 2 (WO_3/Ag/W/WO_3, 50/10/3/50 nm), WAW 3 (WO_3/Ag/W/WO_3, 75/10/3/75 nm), WAW 4 (WO_3/Ag/W/WO_3, 100/10/3/100 nm), and WAW 5 (WO_3/Ag/W/WO_3, 125/10/3/125 nm).

3. Materials and characterization

The deposited WAW films have been carefully characterized. Raman and XRD were used to examine the structural characteristics (Rigaku-MiniFlex). A UV–vis spectrometer (SPECORD S600, Analytikzena) was used to record the optical transmittance spectra of WAW thin films in the 200–1100 nm range. Using an electrochemical analyzer, the electrochromic behavior of WAW thin films was investigated This electrochemical device includes a three-electrode configuration (SP-300, Biologic) with platinum, $Hg_2/HgCl_2$, and WAW thin film electrodes are counter electrode, reference electrode and working electrode respectively. The CV tests were conducted in a solution with a concentration of 0.5 M of H_2SO_4, using potential ranges from -1 V to 1 V, and a scan rate of 30 mVs^{-1} was used.

4. Results and discussions

4.1. XRD analysis

Fig. 2. shows the XRD results of WAW 4 and WAW 5 thin films deposited by using DC and RF magnetron sputtering at RT. The figure shows the diffraction peaks of crystalline Ag metal. The diffraction angle 2θ values are 29.08° of (001), 35.77° of (100), 39.05° of (111), 42.89° of (220), 47.17° of (200), and 48.27° of (211). The crystallite size (D) of the WO_3 films was calculated by using Debye–Scherrer's relation shown in the equation.

$$D = \frac{0.96\ \lambda}{\beta cos\theta} \tag{1}$$

Where θ, β, and λ, are the diffraction angle, FWHM, and wavelength. The calculated Full width at half maximum (FWHM) and crystallite sizes of WAW 4 and WAW 5 are 27.72° and 0.6 nm respectively [71–75]. It's worth noting that none of the patterns show any WO_3 peaks, indicating that the WO_3 layer was amorphous under the deposition conditions, which is good for EC performance [33]. The possible reason is that during the process of depositing the coating layer, the oxygen of the reaction gas flowing into the chamber was dissociated into oxygen ions by the plasma, and the silver was easily combined with oxygen, yet the active oxygen ions were made before the deposition of the tungsten oxide.

4.2. Raman analysis

Raman spectroscopy was used to characterize the crystalline nature and chemical bonding of the WAW films deposited by using DC and RF magnetron sputtering shown in Fig. 3. Raman spectra of WO_3 thin films show two broad bands, one is lower frequency and another higher frequency ie 200–400 cm^{-1} and 700–1000 cm^{-1}. In the low-frequency region, the band observed at around 241 cm^{-1} is attributed to δ (O-W-O). At higher frequencies, broad Raman peaks were observed at around 943 cm^{-1} and 771 cm^{-1} attributed to stretching mode vibration modes of the bridging oxygen $W = O$ and O-W-O, respectively.

4.3. Optical properties

The thickness of each layer has a significant impact on the optical and electrical properties of stacked WAW films. The films have a thin but continuous center metal layer that ensures low absorption and sheet resistance. High transmittance and great EC performance would be possible if the inner and outer dielectric layers were of sufficient thickness. The optical transmittance of WAW thin film structure with different thicknesses is shown in Fig. 4. The transmittance varied from 73%, 61%, 64%, 55%, and 43% at a wavelength of 600 nm. Fig. 2 shows the WAW 3 structure shows the higher the transmittance and the lower at WAW 5. We have deposited the WO_3 thin film layer on the glass substrate as a bottom layer, on top of the silver layer was coated. To

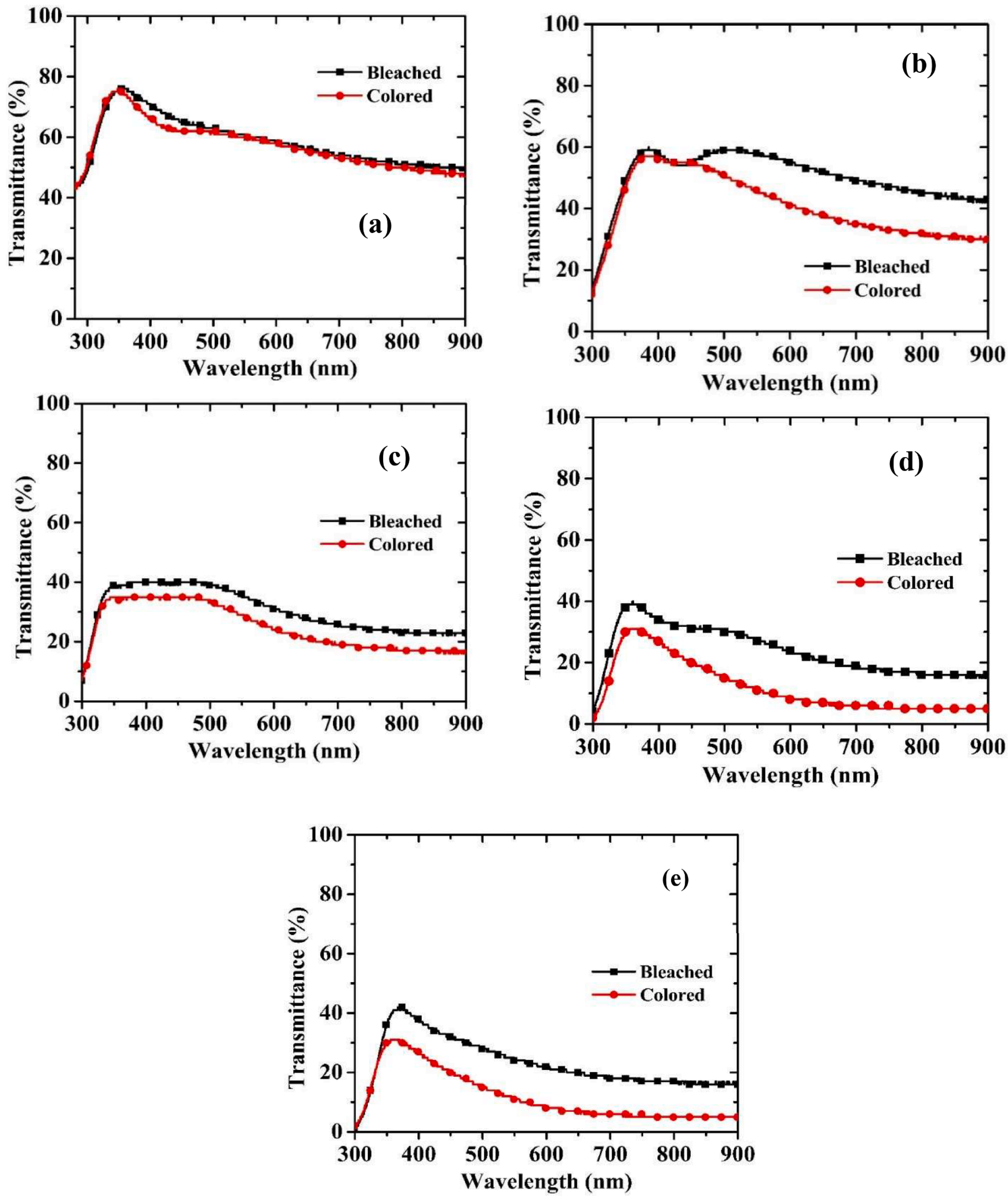

Fig. 7. bleached and colored states of (a) WAW 1, (b) WAW 2, (c) WAW 3 (d) WAW 4 and (e) WAW 5 structure.

avoid the silver oxidation, we have introduced a sacrificial layer of the tungsten metal layer with a fixed thickness, then we have coated the top layer of WO_3 thin film. We have observed that without a sacrificial layer of tungsten metal, the entire device is insulating and it is not working due to the oxidation of silver and the conductivity of the silver decrease. we can see that as we increase on top and bottom layer thickness the transmittance was decreased with a fixed thickness of Ag and W. The calculated bandgap values are 3.20 eV, 2.83 eV, 3.32 eV, 3.39 eV, and 3.25 eV for WAW-1, WAW-2, WAW-3, WAW-4, and WAW-5 respectively. The calculated sheet resistance is 16.75, 16.28, 15.45, 13.25 and 14.4 Ω/□ for WAW-1, WAW-2, WAW-3, WAW-4, and WAW-5 respectively [76,77].

4.4. Electrochemical studies

Fig. 5 shows the Cyclic Voltammetry (CV) plots of WAW thin films deposited by using DC and RF magnetron sputtering on corning glass substrate at room temperature. The electrochromic studies were done by using a programmable three-electrode electrochemical setup. The electrodes are WE as WAW, RE as Hg/Hg_2Cl_2, and AE as platinum wire. The CV analysis was done with the electrolyte of 0.5 M of H_2SO_4 and with a scan rate of 30 mVs^{-1} in the potential range of ± 1 V. From CV plots the

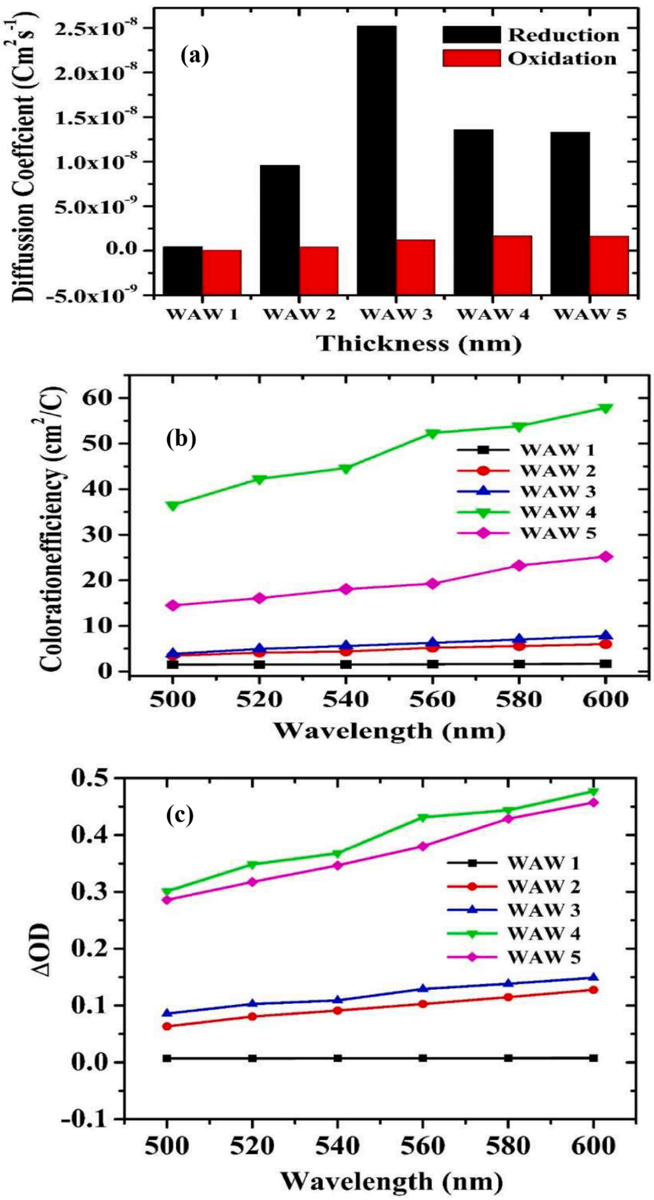

Fig. 8. (a) Diffusion Coefficient, (b) Coloration efficiency, and (c) optical density of WAW structure.

reduction current was shown as 1.11 mA, 5.09 mA, 8.27 mA, 6.10 mA, and 6.01 mA for WAW-1 to WAW-5 respectively. A higher reduction current was shown in the sample WAW-3.

Fig. 6. (a & b) show the charge and current density vs tim0e plots of the WAW structures and observed high values for both the charge and current density for the WAW-3 structure. The transmittance for the bleached and colored state of the WAW structure is shown in Fig. 7. The observed bleached transmittance values are 58%, 55%, 31%, 24%,22% and colored transmittance values are 56%, 41%, 22%, 2%, and 7% for WAW-1 to WAW-5 respectively. From these transmittance results, the optical modulation was shown higher for WAW-4. The diffusion coefficient plots of the WAW structure are shown in Fig. 7(a). It is varied from 4.54×10^{-10}, 9.54×10^{-9}, 2.52×10^{-8}, 1.35×10^{-8} and 1.33×10^{-8} cm^2s^{-1} for WAW-1 to WAW-5 respectively, and the higher diffusion coefficient was observed in WAW-3 structure. The coloration efficiency (CE) of the WAW structure is shown in Fig. 7(b). It varied from 1.6, 5.88, 7.8, 57.87, and 25.19 cm^2C^{-1} for WAW-1 to WAW-5 respectively at the wavelength of 600 nm and the higher CE was observed in the WAW-4 structure [78,79], (Fig. 8).

5. Conclusions

Indium-free transparent WAW thin films have been successfully deposited by using the DC and RF magnetron sputtering. The structural, optical, and electrochromic properties of WAW thin films were systematically analyzed. From the optical transmittance data, transmittance varied from 73%, 61%, 64%, 55%, and 43% with respect to the thickness of the WAW thin film was observed. From electrochemical analysis higher current and diffusion coefficients were observed for WAW 3 thin film. The coloration efficiency was observed at 57.87 cm^2C^{-1}.

Funding

The authors thank the Researchers Supporting Project number (RSP2024R169), King Saud University, Riyadh, Saudi Arabia for the financial support.

Ethical approval

Not Applicable

CRediT authorship contribution statement

K Naveen Kumar: Methodology, Investigation, Funding acquisition. **Habibuddin Shaik:** Validation, Methodology, Investigation, Funding acquisition. **Sheik Abdul Sattar:** Validation, Methodology, Investigation, Funding acquisition. **Ashok Reddy G V:** . **Ramanadha Mangiri:** Validation, Investigation. **R Imran Jafri:** Validation, Methodology, Investigation, Funding acquisition. **R. Premkumar:** Validation, Investigation. **R. Govindharaju:** Investigation, Validation, Writing – review & editing. **B. Mary Juliet:** Investigation, Validation, Writing – review & editing. **Sabah Ansar:** Writing – review & editing.

Declaration of competing interest

The authors declare that they have no known competing financial interests or personal relationships that could have appeared to influence the work reported in this paper.

Data availability

The data that has been used is confidential.

Acknowledgement

The author acknowledges AICTE for financial support, the project Ref: 8–39/RIFD/RPS/POLICY-1/2016–2017, and the authors thank the Researchers Supporting Project number (RSP2024R169), King Saud University, Riyadh, Saudi Arabia for the financial support.

References

[1] C.G. Granqvist, Transparent conductors as solar energy materials: a panoramic review, Solar Energy Materials and Solar Cells 91 (2007) 1529–1598, https://doi.org/10.1016/j.solmat.2007.04.031.
[2] Z. Wang, X. Cai, Q. Chen, P.K. Chu, Effects of Ti transition layer on stability of silver/titanium dioxide multilayered structure, Thin Solid Films 515 (2007) 3146–3150, https://doi.org/10.1016/j.tsf.2006.08.040.
[3] C.G. Granqvist, A. Hultåker, Transparent and conducting ITO films: new developments and applications, Thin Solid Films 411 (2002) 1–5, https://doi.org/10.1016/S0040-6090(02)00163-3.
[4] C.Y. Hsu, L.M. Kao, Y.C. Lin, Effect of deposition parameters and annealing temperature on the structure and properties of Al-doped ZnO thin films, Mater Chem Phys 124 (2010) 330–335, https://doi.org/10.1016/j.matchemphys.2010.06.042.
[5] K. Tominaga, M. Kataoka, T. Ueda, M. Chong, Y. Shintani, I. Mori, Preparation of conductive ZnO:al films by a facing target system with a strong magnetic field,

Thin Solid Films 253 (1994) 9–13, https://doi.org/10.1016/0040-6090(94)90285-2.
[6] H. Kim, J.S. Horwitz, S.B. Qadri, D.B. Chrisey, Epitaxial growth of Al-doped ZnO thin films grown by pulsed laser deposition, Thin Solid Films 420–421 (2002) 107–111, https://doi.org/10.1016/S0040-6090(02)00658-2.
[7] X. jing Wang, Q. song Lei, W. Xu, W. li Zhou, J. Yu, Preparation of ZnO:al thin film on transparent TPT substrate at room temperature by RF magnetron sputtering technique, Mater Lett 63 (2009) 1371–1373, https://doi.org/10.1016/j.matlet.2008.12.027.
[8] J. Hu, R.G. Gordon, Deposition of Boron Doped Zinc Oxide Films and Their Electrical and Optical Properties, J Electrochem Soc 139 (1992) 2014–2022, https://doi.org/10.1149/1.2221166.
[9] B.N. Pawar, S.R. Jadkar, M.G. Takwale, Deposition and characterization of transparent and conductive sprayed ZnO:b thin films, Journal of Physics and Chemistry of Solids 66 (2005) 1779–1782, https://doi.org/10.1016/j.jpcs.2005.08.086.
[10] Y.H. Kim, J. Jeong, K.S. Lee, B. Cheong, T.Y. Seong, W.M. Kim, Effect of composition and deposition temperature on the characteristics of Ga doped ZnO thin films, Appl Surf Sci 257 (2010) 109–115, https://doi.org/10.1016/j.apsusc.2010.06.045.
[11] H.S. Yoon, K.S. Lee, T.S. Lee, B. Cheong, D.K. Choi, D.H. Kim, W.M. Kim, Properties of fluorine doped ZnO thin films deposited by magnetron sputtering, Solar Energy Materials and Solar Cells 92 (2008) 1366–1372, https://doi.org/10.1016/j.solmat.2008.05.010.
[12] J. Lee, E. Park, N.G. Subramaniam, J. Lee, J. Lee, J. Lee, T. Kang, Non-metallic element (chlorine) doped Zinc oxide grown by pulsed laser deposition for application in transparent electrode, Current Applied Physics 12 (2012) S80–S84, https://doi.org/10.1016/j.cap.2012.05.019.
[13] J. Do Yang, S.H. Cho, T.W. Hong, D.I. Son, D.H. Park, K.H. Yoo, W.K. Choi, Organic photovoltaic cells fabricated on a SnO x/Ag/SnO x multilayer transparent conducting electrode, Thin Solid Films 520 (2012) 6215–6220, https://doi.org/10.1016/j.tsf.2012.05.029.
[14] P.K. Chiu, D. Chiang, W.H. Cho, C.N. Hsiao, Y.Y. Chen, B.M. Huang, J.R. Yang, Conductive and transparent multilayer films for low-temperature Tio2/Ag/SiO2 electrodes by E-beam evaporation with IAD, Nanoscale Res Lett 9 (2014) 1–8, https://doi.org/10.1186/1556-276X-9-35.
[15] Z. Qi, J. Cao, L. Ding, J. Wang, Transparent and transferrable organic optoelectronic devices based on WO3/Ag/WO3 electrodes, Appl Phys Lett 106 (2015), https://doi.org/10.1063/1.4907865.
[16] X. Liu, X. Cai, J. Qiao, J. Mao, N. Jiang, The design of ZnS/Ag/ZnS transparent conductive multilayer films, Thin Solid Films 441 (2003) 200–206, https://doi.org/10.1016/S0040-6090(03)00141-X.
[17] Y. Liu, Y. Lv, Z. Tang, L. He, X. Liu, Highly stable and flexible ITO-free electrochromic films with bi-functional stacked MoO3/Ag/MoO3 structures, Electrochim Acta 189 (2016) 184–189, https://doi.org/10.1016/j.electacta.2015.12.115.
[18] A. Dhar, T.L. Alford, High quality transparent TiO2/Ag/TiO2 composite electrode films deposited on flexible substrate at room temperature by sputtering, APL Mater 1 (2013), https://doi.org/10.1063/1.4808438.
[19] E. Koubli, S. Tsakanikas, G. Leftheriotis, G. Syrrokostas, P. Yianoulis, Optical properties and stability of near-optimum WO3/Ag/WO3 multilayers for electrochromic applications, Solid State Ion 272 (2015) 30–38, https://doi.org/10.1016/j.ssi.2014.12.015.
[20] A. Ghicov, S.P. Albu, J.M. Macak, P. Schmuki, High-contrast electrochromic switching using transparent lift-off layers of self-organized TiO2 nanotubes, Small 4 (2008) 1063–1066, https://doi.org/10.1002/smll.200701244.
[21] M.S. Wu, C.H. Yang, Electrochromic properties of intercrossing nickel oxide nanoflakes synthesized by electrochemically anodic deposition, Appl Phys Lett 91 (2007), https://doi.org/10.1063/1.2759270.
[22] K.C. Cheng, F.R. Chen, J.J. Kai, V2O5 nanowires as a functional material for electrochromic device, Solar Energy Materials and Solar Cells 90 (2006) 1156–1165, https://doi.org/10.1016/j.solmat.2005.07.006.
[23] S.J. Yoo, J.W. Lim, Y.E. Sung, Y.H. Jung, H.G. Choi, D.K. Kim, Fast switchable electrochromic properties of tungsten oxide nanowire bundles, Appl Phys Lett 90 (2007) 88–91, https://doi.org/10.1063/1.2734395.
[24] J. Gupta, H. Shaik, K.N. Kumar, A review on the prominence of porosity in tungsten oxide thin films for electrochromism, Ionics (Kiel) 27 (2021) 2307–2334, https://doi.org/10.1007/s11581-021-04035-8.
[25] J. Gutpa, H. Shaik, K.N. Kumar, S. Abdul, Materials Science in Semiconductor Processing PVD techniques proffering avenues for fabrication of porous tungsten oxide (WO 3) thin films : a review, Mater Sci Semicond Process 143 (2022) 106534, https://doi.org/10.1016/j.mssp.2022.106534.
[26] R. Cinnsealach, G. Boschloo, S.N. Rao, D. Fitzmaurice, Electrochromic windows based on viologen-modified nanostructured TiO2 films, Solar Energy Materials and Solar Cells 55 (1998) 215–223, https://doi.org/10.1016/S0927-0248(98)00096-8.
[27] P. Andersson, R. Forchheimer, P. Tehrani, M. Berggren, Printable all-organic electrochromic active-matrix displays, Adv Funct Mater 17 (2007) 3074–3082, https://doi.org/10.1002/adfm.200601241.
[28] N. Gospodinova, L. Terlemezyan, Conducting polymers prepared by oxidative polymerization: polyaniline, Progress in Polymer Science (Oxford) 23 (1998) 1443–1484, https://doi.org/10.1016/S0079-6700(98)00008-2.
[29] M. Rao, Structure and properties of WO3 thin films for electrochromic device application, J. Non-Oxide Glasses 5 (2013) 1–8.
[30] M. Bourdin, G. Salek, A. Fargues, S. Messaddeq, Y. Messaddeq, T. Cardinal, M. Gaudon, Investigation on the coloring and bleaching processes of WO3-xphotochromic thin films, J Mater Chem C Mater 8 (2020) 9410–9421, https://doi.org/10.1039/d0tc02170a.
[31] A. Mirzaei, J.H. Kim, H.W. Kim, S.S. Kim, Gasochromic WO3 nanostructures for the detection of hydrogen gas: an overview, Applied Sciences (Switzerland) 9 (2019), https://doi.org/10.3390/app9091775.
[32] C.V. Ramana, A.K. Battu, P. Dubey, G.A. Lopez, Phase-Control-Enabled Enhancement in Hydrophilicity and Mechanical Toughness in Nanocrystalline Tungsten Oxide Films for Energy-Related Applications, ACS Appl Nano Mater 3 (2020) 3264–3274, https://doi.org/10.1021/acsanm.9b02576.
[33] P.M.S. Monk, D.R. Rosseinsky, R.J. Mortimer, Electrochromic Materials and Devices Based on Viologens, Electrochromic Materials and Devices 77 (2015) 57–90, https://doi.org/10.1002/9783527679850.ch3.
[34] R. Sivakumar, K. Shanthakumari, A. Thayumanavan, M. Jayachandran, C. Sanjeeviraja, Coloration and bleaching mechanism of tungsten oxide thin films in different electrolytes, Surface Engineering 23 (2007) 373–379, https://doi.org/10.1179/174329407X247181.
[35] J. Gupta, H. Shaik, K.N. Kumar, S.A. Sattar, G.V.A. Reddy, Optimization of deposition rate for E-beam fabricated tungsten oxide thin films towards profound electrochromic applications, Appl Phys A Mater Sci Process 128 (2022), https://doi.org/10.1007/s00339-022-05609-7.
[36] J. Gutpa, H. Shaik, K. Naveen Kumar, S.A. Sattar, Optimization of GLAD Angle for E-Beam-Fabricated Tungsten Oxide (WO3) Thin Films Towards Novel Electrochromic Behavior, J Electron Mater 52 (2023) 653–668, https://doi.org/10.1007/s11664-022-10036-8.
[37] M.F. Al-Kuhaili, A.H. Al-Aswad, S.M.A. Durrani, I.A. Bakhtiari, Transparent heat mirrors based on tungsten oxide-silver multilayer structures, Solar Energy 83 (2009) 1571–1577, https://doi.org/10.1016/j.solener.2009.05.006.
[38] T. Polcar, N.M.G. Parreira, A. Cavaleiro, Tungsten oxide with different oxygen contents: sliding properties, Vacuum 81 (2007) 1426–1429, https://doi.org/10.1016/j.vacuum.2007.04.001.
[39] I. Valyukh, S. Green, H. Arwin, G.A. Niklasson, E. Wäckelgård, C.G. Granqvist, Spectroscopic ellipsometry characterization of electrochromic tungsten oxide and nickel oxide thin films made by sputter deposition, Solar Energy Materials and Solar Cells 94 (2010) 724–732, https://doi.org/10.1016/j.solmat.2009.12.011.
[40] R. Figueroa, M. Kleinke, T.G.S. Cruz, A. Gorenstein, Influence of the microstructure on the electrochemical performance of thin film WO3 cathode, J Power Sources 162 (2006) 1351–1356, https://doi.org/10.1016/j.jpowsour.2006.08.002.
[41] K. Naveen Kumar, H. Shaik, V.Madhavi Sathish, S. Abdul Sattar, On the Bonding and Electrochemical Performance of Sputter Deposited WO3 Thin Films, IOP Conf Ser Mater Sci Eng 872 (2020), https://doi.org/10.1088/1757-899X/872/1/012147.
[42] K. Naveen Kumar, H. Shaik, V.Madhavi Sathish, S. Abdul Sattar, On the Bonding and Electrochemical Performance of Sputter Deposited WO3 Thin Films. IOP Conf Ser Mater Sci Eng, Institute of Physics Publishing, 2020, https://doi.org/10.1088/1757-899X/872/1/012147.
[43] V. Madhavi, P. Kondaiah, H. Shaik, K.N. Kumar, T.S.S. Kumar Naik, G.M. Rao, P. C. Ramamurthy, Fabrication of porous 1D WO3 NRs and WO3/BiVO4 hetero junction photoanode for efficient photoelectrochemical water splitting, Mater Chem Phys 274 (2021), https://doi.org/10.1016/j.matchemphys.2021.125095.
[44] K.N. Kumar, G. Nithya, H. Shaik, L.N. Chandrashekar, P. Aishwarya, A.S. Pawar, Optical and electrochromic properties of DC magnetron sputter deposited tungsten oxide thin films at different electrolyte concentrations and vertex potentials for smart window applications, Journal of Materials Science: Materials in Electronics 34 (2023), https://doi.org/10.1007/s10854-023-10180-9.
[45] G.V. Ashok Reddy, K.N. Kumar, R. Naik, V. Revathi, K.M. Girish, K. Munirathnam, Comparative analysis of the effect of post-annealing on CeO2 and DC Magnetron Sputtered WO3/CeO2 nanorods thin films for smart windows, Applied Surface Science Advances 16 (2023), https://doi.org/10.1016/j.apsadv.2023.100417.
[46] A.R.G. V, K.N. Kumar, H.D. Shetty, C. Devaraja, M. Dhananjaya, S.M. Hunagund, Materials Today : proceedings Comparison study of WO 3 thin film and nanorods for smart window applications, Mater Today Proc (2023), https://doi.org/10.1016/j.matpr.2023.03.052.
[47] A.R.G. V, H. Shaik, K.N. Kumar, V. Madhavi, H.D. Shetty, S.A. Sattar, M. Dhananjaya, B. Daruka Prasad, G.R. Kumar, B.H. Doreswamy, Structural and electrochemical studies of WO3 coated TiO2 nanorod hybrid thin films for electrochromic applications, Optik (Stuttg) 277 (2023), https://doi.org/10.1016/j.ijleo.2023.170694.
[48] A.R.G. V, H. Shaik, K. Naveen Kumar, R. Imran Jafri, S. Abdul Sattar, J. Gupta, B. H. Doreswamy, Thickness dependent tungsten trioxide thin films deposited using DC magnetron sputtering for electrochromic applications, Mater Today Proc 80 (2023) 817–823, https://doi.org/10.1016/j.matpr.2022.11.134.
[49] K. Naveen Kumar, H. Shaik, V. Madhavi, R. Imran Jafri, J. Gupta, G. Nithya, S. A. Sattar, G.V. Ashok Reddy, Glancing angle sputter deposited tungsten trioxide (WO3) thin films for electrochromic applications, Appl Phys A Mater Sci Process 128 (2022), https://doi.org/10.1007/s00339-022-06124-5.
[50] K.N. Kumar, H. Shaik, J. Gupta, S. Abdul, I. Jafri, A. Pawar, V. Madhavi, A.R.G. V, G. Nithya, Sputter deposited tungsten oxide thin films and nanopillars : electrochromic perspective, Mater Chem Phys 278 (2022) 125706, https://doi.org/10.1016/j.matchemphys.2022.125706.
[51] K. Naveen Kumar, H. Shaik, A. Pawar, L.N. Chandrashekar, S.A. Sattar, G. Nithya, R. Imran Jafri, V. Madhavi, J. Gupta, G.V. Ashok Reddy, Effect of annealing and oxygen partial pressure on the RF sputtered WO3 thin films for electrochromic applications, Mater Today Proc (2021), https://doi.org/10.1016/j.matpr.2021.11.185.
[52] K. Naveen Kumar, H. Shaik, L.N. Chandrashekar, P. Aishwarya, S. Abdul Sattar, G. Nithya, V. Madhavi, R. Imran Jafri, J. Gupta, G.V. Ashok Reddy, On ion

transport during the electrochemical reaction on plane and GLAD deposited WO3 thin films, Mater Today Proc (2021), https://doi.org/10.1016/J.MATPR.2021.11.113.
[53] K. Naveen Kumar, H. Shaik, A. Pawar, L.N. Chandrashekar, S.A. Sattar, G. Nithya, R. Imran Jafri, V. Madhavi, J. Gupta, G.V. Ashok Reddy, Effect of annealing and oxygen partial pressure on the RF sputtered WO3 thin films for electrochromic applications, Mater Today Proc 59 (2022) 339–344, https://doi.org/10.1016/j.matpr.2021.11.185.
[54] K. Naveen Kumar, G. Nithya, H. Shaik, B. Hemanth, M. Chethana, K. Kishore, V. Madhavi, R.I. Jafri, S.A. Sattar, J. Gupta, G.V. Ashok Reddy, Simulation and fabrication of tungsten oxide thin films for electrochromic applications, Physica B Condens Matter 640 (2022), https://doi.org/10.1016/j.physb.2022.413932.
[55] K.N. Kumar, S.A. Sattar, G.V. Ashok Reddy, R.I. Jafri, R. Premkumar, M.R. Meera, A.A. Ahamed, M. Muthukrishnan, M. Dhananjaya, A.M. Tighezza, Structural, optical, and electrochromic properties of RT and annealed sputtered tungsten trioxide (WO3) thin films for electrochromic applications by using GLAD technique, Journal of Materials Science: Materials in Electronics 34 (2023), https://doi.org/10.1007/s10854-023-11285-x.
[56] A.R.G. V, K.N. Kumar, S. Abdul, H.D. Shetty, N. Guru, R.I. Jafri, C. Devaraja, B. C. Manjunatha, C.S. Kaliprasad, R. Premkumar, S. Ansar, Physica B : condensed Matter Effect of post annealing on DC magnetron sputtered tungsten oxide (WO 3) thin films for smartwindow applications, Physica B Condens Matter 664 (2023) 414996, https://doi.org/10.1016/j.physb.2023.414996.
[57] K.N. Kumar, S.A. Sattar, H. Shaik, A.R.G. V, R.I. Jafri, M. Dhananjaya, A.S. Pawar, N.G. Prakash, R. Premkumar, S. Ansar, L.N. Chandrashekar, P. Aishwarya, Effect of partial pressure of oxygen, target current, and annealing on DC sputtered tungsten oxide (WO3) thin films for electrochromic applications, Solid State Ion 399 (2023), https://doi.org/10.1016/j.ssi.2023.116275.
[58] G.V. Ashok Reddy, K. Naveen Kumar, H.D. Shetty, C. Devaraja, M. Dhananjaya, H. B. Shiva prased, N.G. Prakash, K.M. Girish, A.R. Venugopal, K. Deepak, S. M. Hunagund, Comparison study of WO3 thin film and nanorods for smart window applications, Mater Today Proc (2023), https://doi.org/10.1016/j.matpr.2023.03.052.
[59] J. Zhang, X.L. Wang, X.H. Xia, C.D. Gu, J.P. Tu, Solar Energy Materials & Solar Cells Electrochromic behavior of WO 3 nanotree films prepared by hydrothermal oxidation, 95 (2011) 2107–2112. 10.1016/j.solmat.2011.03.008.
[60] A.G.V. Reddy, K.N. Kumar, H. Shaik, R.I. Jafri, R. Naik, B.H. Doreswamy, Optical and Electrochromic Properties of CeO2/WO3 Hybrid Thin Films Prepared by Hydrothermal and Sputtering, International Journal of Engineering Trends and Technology 70 (2022) 1–8, https://doi.org/10.14445/22315381/IJETT-V70I5P201.
[61] G.V.A. Reddy, K.N. Kumar, R. Naik, V. Revathi, K.M. Girish, K. Munirathnam, Applied Surface Science Advances Comparative analysis of the effect of post-annealing on CeO 2 and DC Magnetron Sputtered WO 3 /CeO 2 nanorods thin films for smart windows, Applied Surface Science Advances 16 (2023) 100417, https://doi.org/10.1016/j.apsadv.2023.100417.
[62] G.V.A. Reddy, S. Abdul Sattar, K.N. Kumar, B.D. Prasad, C. Devaraja, H. S. Yogananda, Effect of growth fluid concentration on characteristics of CeO2 nanorods and WO3/CeO2 nanostructured hybrid films for electrochromic applications, Journal of Materials Science: Materials in Electronics 34 (2023), https://doi.org/10.1007/s10854-023-10850-8.
[63] A.R.G. V., K.N. Kumar, H. Shaik, R.I. Jafri, R. Naik, B.H. Doreswamy, Optical and Electrochromic Properties of CeO 2 /WO 3 Hybrid Thin Films Prepared by Hydrothermal and Sputtering, 70 (2022) 1–8.
[64] G.V. Ashok Reddy, K.N. Kumar, S.A. Sattar, N.G. Prakash, B. Daruka Prasad, M. Dhananjaya, G.R. Kumar, H.S. Yogananda, S.M. Hunagund, S. Ansar, Structural, optical, and electrochromic properties of rare earth material (CeO2)/transitional metal oxide (WO3) thin film composite structure for electrochromic applications, Ionics (Kiel) (2023), https://doi.org/10.1007/s11581-023-05078-9.
[65] G.V. Ashok Reddy, S.A. Sattar, K. Naveen Kumar, C.S. KaliPrasad, C. Devaraja, R. Imran Jafri, B.H. Doreswamy, Effect of tungsten oxide thin films deposited on cerium oxide nano rods for electrochromic applications, Opt Mater (Amst) 134 (2022), https://doi.org/10.1016/j.optmat.2022.113220.
[66] G.V. Ashok Reddy, H. Shaik, K.N. Kumar, H.D. Shetty, R.I. Jafri, R. Naik, J. Gupta, S.A. Sattar, B.H. Doreswamy, Synthesis, characterizations, and electrochromic studies of WO3 coated CeO2 nanorod thin films for smart window applications, Physica B Condens Matter 647 (2022), https://doi.org/10.1016/j.physb.2022.414395.
[67] C. Zhang, M. Debliquy, A. Boudiba, H. Liao, C. Coddet, Sensing properties of atmospheric plasma-sprayed WO3 coating for sub-ppm NO2 detection, Sens Actuators B Chem 144 (2010) 280–288, https://doi.org/10.1016/j.snb.2009.11.006.
[68] X. Sun, H. Cao, Z. Liu, J. Li, Influence of annealing temperature on microstructure and optical properties of sol-gel derived tungsten oxide films, Appl Surf Sci 255 (2009) 8629–8633, https://doi.org/10.1016/j.apsusc.2009.06.042.
[69] S. Yang, Y. Tang, T. Ta, W. Li, Q. Wang, S. Yang, B. Zou, Transparent WO3/Ag/WO3 electrode for flexible organic solar cells, Mater Lett 188 (2017) 107–110, https://doi.org/10.1016/j.matlet.2016.11.054.
[70] K. Hong, K. Kim, S. Kim, I. Lee, H. Cho, S. Yoo, H.W. Choi, N.Y. Lee, Y.H. Tak, J. L. Lee, Optical properties of WO3/Ag/WO3 multilayer as transparent cathode in top-emitting organic light emitting diodes, Journal of Physical Chemistry C 115 (2011) 3453–3459, https://doi.org/10.1021/jp109943b.
[71] L.H. Abdel Rahman, A.M. Abu-Dief, R.M. El-Khatib, S.M. Abdel-Fatah, A.M. Adam, E.M.M. Ibrahim, Sonochemical synthesis, structural inspection and semiconductor behavior of three new nano sized Cu(II), Co(II) and Ni(II) chelates based on tri-dentate NOO imine ligand as precursors for metal oxides, Appl Organomet Chem 32 (2018), https://doi.org/10.1002/aoc.4174.
[72] E.M.M. Ibrahim, A.M. Abu-Dief, A. Elshafaie, A.M. Ahmed, Electrical, thermoelectrical and magnetic properties of approximately 20-nm Ni-Co-O nanoparticles and investigation of their conduction phenomena, Mater Chem Phys 192 (2017) 41–47, https://doi.org/10.1016/j.matchemphys.2017.01.054.
[73] E.M.M. Ibrahim, L.H. Abdel-Rahman, A.M. Abu-Dief, A. Elshafaie, S.K. Hamdan, A. M. Ahmed, The synthesis of CuO and NiO nanoparticles by facile thermal decomposition of metal-Schiff base complexes and an examination of their electric, thermoelectric and magnetic Properties, Mater Res Bull 107 (2018) 492–497, https://doi.org/10.1016/j.materresbull.2018.08.020.
[74] E.M.M. Ibrahim, L.H. Abdel-Rahman, A.M. Abu-Dief, A. Elshafaie, S.K. Hamdan, A. M. Ahmed, Electric, thermoelectric and magnetic characterization of γ-Fe2O3 and Co3O4 nanoparticles synthesized by facile thermal decomposition of metal-Schiff base complexes, Mater Res Bull 99 (2018) 103–108, https://doi.org/10.1016/j.materresbull.2017.11.002.
[75] M. Alahmadi, W.H. Alsaedi, W.S. Mohamed, H.M.A. Hassan, M. Ezzeldien, A. M. Abu-Dief, Development of Bi2O3/MoSe2 mixed nanostructures for photocatalytic degradation of methylene blue dye, Journal of Taibah University for Science 17 (2023), https://doi.org/10.1080/16583655.2022.2161333.
[76] W.S. Mohamed, N.M.A. Hadia, B. Al bakheet, M. Alzaid, A.M. Abu-Dief, Impact of Cu2+ cations substitution on structural, morphological, optical and magnetic properties of Co1-xCuxFe2O4 nanoparticles synthesized by a facile hydrothermal approach, Solid State Sci 125 (2022) 106841, https://doi.org/10.1016/J.SOLIDSTATESCIENCES.2022.106841.
[77] M. Alzaid, W.S. Mohamed, R. Alanazi, I.H. Alsohaimi, H.M.A. Hassan, N.M. A. Hadia, M. Ezzeldien, M.R. El-Aassar, A.M. Abu-Dief, Novel (Y2O3) x (CdO) 1-x binary mixed oxide nanocomposites: facile synthesis, characterization, and photocatalysis enhancement, Journal of Materials Research and Technology 23 (2023) 2454–2466, https://doi.org/10.1016/j.jmrt.2023.01.105.
[78] E.S. Al-Farraj, M. Alahmadi, W.S. Mohamed, W.H. Alsaedi, A.M. Abu-Dief, Development of VSe_2 @ Cu_2Se nano-composites via facile one-pot hydrothermal method for pharmaceutical applications, Phys Scr 98 (2023) 095004, https://doi.org/10.1088/1402-4896/aceada.
[79] M.A. Awad, A.M. Abu-Dief, Tuning the luminescence performance of CdO nanoparticles via Tb_2O_3 inclusion, Phys Scr 97 (2022) 085811, https://doi.org/10.1088/1402-4896/ac7e7f.